SOME RECENT APPLICATIONS OF NAVIER-STOKES CODES TO ROTORCRAFT

W.J. McCroskey

Senior Research Scientist
U.S. Army Aeroflightdynamics Directorate (AVSCOM)
and NASA Ames Research Center
Moffett Field, California

ABSTRACT

Many operational limitations of helicopters and other rotary-wing aircraft are due to nonlinear aerodynamic phenomena, including unsteady, three-dimensional transonic and separated flow near the surfaces and highly vortical flow in the wakes of rotating blades. Modern computational fluid dynamics (CFD) technology offers new tools to study and simulate these complex flows. However, existing Euler and Navier-Stokes codes have to be modified significantly for rotorcraft applications, and the enormous computational requirements presently limit their use in routine design applications. Nevertheless, the Euler/Navier-Stokes technology is progressing in anticipation of future supercomputers that will enable meaningful calculations to be made for complete rotorcraft configurations.

I. INTRODUCTION

The flow fields of helicopters and other rotorcraft provide a rich variety of challenging problems in applied aerodynamics. Much of the flow near the rotating blades is nonlinear, three-dimensional, and often unsteady, with periodic regions of transonic flow near the blade tips, and with dynamic stall pockets inboard. The blades also shed complex vortical wakes, and detrimental aerodynamic interactions often arise between the major rotating and nonrotating components.

In recent years, CFD methods for isolated, nonlinear pieces of the overall problem have been developed to complement the mixture of analytical and empirical aerodynamic theories, wind tunnel data, and design charts traditionally used by helicopter engineers. References 1-4, for example, describe some of these modern developments, and the present author highlighted the activities of some of his colleagues in Ref. 5, as they existed in 1988. This paper represents a brief review and update of those efforts described in Ref. 5, with some additional discussion of the challenges that remain to our long-term goal of obtaining complete numerical simulations of realistic rotorcraft flow fields with as few physical approximations as possible. It must be emphasized that no attempt is made in this paper to review the bulk of research underway in this field; only the work of the author's immediate colleagues is described herein. Thus, more activities are neglected than included.

As can be gleaned from Refs. 1-5, many different levels of sophistication of CFD technology can be and are being gainfully applied to practical rotorcraft problems. The approach followed here, which is by no means unique (cf. Refs. 4, 6-10), is to develop, adapt, and apply advanced Euler/Reynolds-Averaged Navier-Stokes methodology to the special needs of future rotorcraft. While the near-term utility and practicality of this approach may be open to debate, the history of supercomputer growth and the contributions of advanced CFD techniques to fixed-wing aircraft suggest that improved predictive tools are highly desirable for all flight vehicles. Such methodology should help to reduce the risks and testing requirements for new designs, and it should enable engineers to increase rotorcraft performance, efficiency, and maneuverability while reducing noise, vibrations, and detectability.

In the following section, a very brief description is given of the methods that are currently being developed and used by the author and his coworkers. In subsequent sections, some representative examples of recent results are given, along with descriptions of some of the major issues that remain unresolved.

II. NUMERICAL METHODS

Two different approaches are currently being pursued to solve the compressible Euler or Reynolds-Averaged Thin-Layer Navier-Stokes equations for aerodynamic configurations that consist of rotating lifting surfaces and nonrotating airframe components. The first approach employs several finite-difference, implicit approximate-factorization algorithms, with algebraic turbulence modeling, to solve the governing equations in strong conservation-law form [11] on either single- or multiple-block, body-conforming structured grids. The single-block code is called TURNS (Transonic Unsteady Rotor Navier Stokes), which is described in Ref. 12 and which borrows heavily from Obayashi's work [13]. This numerical scheme uses upwind-biased flux-difference splitting, an LU-SGS implicit operator, higher-order MUSCL-type limiting, and, in the case of unsteady calculations, Newton sub-iterations at each time step.

The current multi-block implicit code is called OVERFLOW, a new code being developed by Dr. Pieter Buning at the Ames Research Center, using elements of F3D [14] and ARC3D [15]. OVERFLOW currently has a two-factor, block tridiagonal option with upwind differencing in the streamwise direction, as in F3D, and a three-factor, scalar pentadiagonal option with central differencing, as in ARC3D. OVERFLOW uses the Chimera overset-grid scheme [16] to subdivide the

Presented at the Fifth Symposium on Numerical and Physical Aspects of Aerodynamic Flows, Long Beach, California, 13-16 January 1992.

computational domain into subdomains, some of which may move relative to others.

Solution-adaptive grids are not currently used in the three-dimensional versions of either TURNS or OVERFLOW, although this technology will be pursued in the future. TURNS has been used to compute the aerodynamics and acoustics of isolated rotor blades, and OVERFLOW has been applied to fuselages and wing-body combinations. The Chimera overset-grid method is currently being combined with TURNS to improve the resolution of vortical structures in the wakes of rotor blades, and OVERFLOW with Chimera is beginning to be applied to rotor-body interactions.

Body-conforming C-O or C-H structured grid topologies are normally used in TURNS and OVERFLOW, with from approximately 100,000 to 1,000,000 grid points. Figure 1 shows a typical C-H grid for aerodynamic calculations. The grid lines are nearly orthogonal at the surface, and the grid spacing normally starts at about 0.00002 - 0.00005 chord in the normal direction. Figure 2 illustrates the distortion of the grid in the H, or spanwise, direction that is typically used for acoustic calculations. For these applications, it is important to align the grid lines with linear characteristics beyond the tip of the rotor, in order to capture the low-level radiating sound waves.

The second approach uses a solution-adaptive unstructured-grid subdivision scheme developed by Strawn [17], incorporating the explicit upwind finite-volume flow solver of Barth [18]. The code contains an efficient edge data structure for computational domains comprised of arbitrary polyhedra, which are subdivided in regions of high flowfield gradients to improve the solution. Barth's method uses a reconstruction scheme in each control volume that is exact for linear variations, and the reconstructed polynomials are flux-limited in regions of flow discontinuities. The explicit time operator is a four-stage Runge-Kutta method with local time stepping for steady problems. The motivation for this adaptive-grid approach is to convect vortical flow regions with minimal numerical dissipation, but it shows promise in convecting low-level acoustic waves, as well. Thus far, only the Euler equations have been solved by this method.

The adaptive-grid calculations normally start on a coarse structured grid. Error indicators, based, for example, on density gradients near the edges of the blade or on vorticity in the wake, determine which tetrahedra volume elements are to be subdivided into eight smaller tetrahedra and which ones are to be left alone. "Buffer" elements consisting of partially subdivided tetrahedra are introduced around the fully-subdivided ones. The process can be repeated until the desired solution accuracy is obtained. References 17-19 may be consulted for details.

III. BLADE AERODYNAMICS AND WAKES

Tip Vortex Formation and Convection

The concentrated tip vortex of a rotor blade plays an important role in the aerodynamics and acoustics of rotary-wing aircraft; even more so than for fixed-wing aircraft, since the tip vortex may stay closer to and directly interact with the rotor or airframe. Calculations of the tip vortex formation and spanwise loading distribution on a rectangular wing tip, performed by Srinivasan, et al [20], were found to be in good overall agreement with experiments, but the computed peak suction levels on the upper surface of the wing very near the tip were not as high as the measured ones, Fig. 3. More recently, Strawn [17] found similar discrepancies in his unstructured-grid calculations. In addition, Strawn found the calculated peak velocities in the vortex itself to be substantially less than recently reported by McAlister and Takahashi [21], although Strawn's computed vortex dissipated very little as it convected downstream. In unpublished work, Srinivasan has re-computed this problem on finer grids with his structured-grid code, with similar results. Thus the cause of the discrepancy remains undetermined, but it appears that even finer grids and/or better turbulence models may be required to resolve this issue. This, in turn, has important implications for the problem of computing rotor blade-vortex interaction accurately, as described below. The tip-vortex formation problem is currently being studied computationally by Dr. Jennifer Dacles-Mariani at the Ames Research Center, in conjunction with a new experimental program [22] designed to shed further light on the physics of this phenomenon.

Despite these limitations, the existing Navier-Stokes technology can provide useful information about the performance of modern blade tips. For example, Duque [23,24] has studied the unusual British Experimental Rotor Program (BERP) helicopter blade under nonrotating conditions, and he has computed the complex separation patterns that develop at high incidence. Figure 4 shows some of these results at low Mach number, in comparison with experimental oil-flow patterns. He also obtained excellent agreement with measured pressure distributions everywhere except in the immediate vicinity of the tip.

Hover

The axial symmetry and nominally steady-state conditions in blade-fixed coordinates make hovering flight of isolated rotor blades an attractive starting point for developing rotorcraft codes. Forerunners of the TURNS code were developed and applied to this problem by Srinivasan, et al [25] and Chen, et al [26]; these efforts were summarized in Ref. 5. Reference 25 showed some of the basic differences between rotating and nonrotating blades, but the induced flow due to the vortical wake was approximated by a simplistic model. However, this restriction was subsequently relaxed by both investigators [12,27], wherein the solution for the wake structure was included, or "captured," as part of the overall computation. Here, as in the fixed-wing tip-vortex problem described above, the vortical wake structure was smeared considerably by the coarseness of the grid and the attendant numerical dissipation. Nevertheless, the circulation and nearfield trajectory of the trailing tip vortex of the blade appeared to be well enough preserved that the induced inflow was computed satisfactorily, thus producing reasonable airloads on the blade. For example, the surface pressure distributions reported in Ref. 12 showed acceptable agreement with experiments. These encouraging results led to recent studies of more complex rotors, as reported in Ref. 28. For example, Fig. 5 shows calculations for the Sikorsky UH-60A main rotor, and Fig. 6 for a blade based on the Westland BERP rotor. The pressure distributions shown in Fig. 5 look very good, although the computed tip vortex structure is smeared and the uncertainty of the calculated induced and profile power of the rotor is greater than today's stringent engineering requirements

for determining hover performance. Therefore, these results should probably only be considered "semi-quantitative." Of course, the issue of the accuracy of drag calculations in three-dimensional applications is not unique to rotorcraft CFD, but it warrants further serious attention for applications such as these.

The ongoing application of the TURNS code to hovering rotors uncovered difficulties with the outer boundary conditions that were not evident at the beginning of the study, and which are still not fully resolved. Unlike a fixed wing, a hovering rotor induces significant velocities at large distances from the rotor. However, for economy, one would like to keep the computational domain as small as possible. In Refs. 12, 25-27, for example, the outer boundaries were placed relatively close to the rotor, and the characteristic far-field boundary conditions that were used effectively blocked flow across the outer surfaces of the computational domain. Thus the problem simulated in those studies was a rotor in a solid-wall enclosure, rather than in free air, and the wake of the rotor tended to recirculate within the computational "box."

This problem, and large time required for the initial transients to decay, were recognized by Kramer, Hertel, and Wagner [29], who used an approximate vortex-element solution to define an initial solution that produced flow through the far-field boundaries. However, a simpler and more economical alternative was introduced in Ref. 28, using simple momentum theory as a guide. Namely, the wake of the rotor was assumed to pass out of the computational box through a circular hole whose area is half that of the rotor disk, with an outflow velocity twice the momentum-theory average value through the plane of the rotor. A characteristic-type numerical outflow boundary condition was applied across this exit plane by prescribing this outflow mass flux, and the other four computational variables were extrapolated from within. The inflow through the rest of the outer boundary was approximated by a point sink at the axis of rotation, whose strength is proportional, again via momentum theory, to the thrust of the rotor. Here the pressure was extrapolated from within and the other four variables were specified. This combination of inflow and outflow boundary conditions is sketched in Fig. 7.

Figure 8 shows a comparison of the pressure distributions on a hovering rotor computed with the old and new outer boundary conditions, from Refs. 12 and 28, respectively. The trace of particles released near the tip, Fig. 9, is assumed to define approximately the trajectory of the tip vortex. The particle trace computed with the new boundary conditions exits the lower computational boundary after about 3-1/2 revolutions of the blade, and this trajectory agrees well with measurements. With the old boundary conditions of no inflow or outflow, the trace is approximately the same for the first 1-1/2 blade revolutions, but then it develops an irregular path that suggests a developing recirculation within the computational domain.

Unfortunately, the pressure distributions in Fig. 8 do not give a clear indication that the new boundary conditions have improved the solution. This is somewhat surprising, and also at variance with the usual results of vortex-element methods, that the airloads seem to be relatively insensitive to the details of the far-wake solutions. As noted earlier, the vortical wake structure of the Navier-Stokes calculations was smeared considerably by the coarseness of the grid away from the blade and the attendant numerical dissipation. However, the circulation and trajectory of the trailing tip vortex through the first revolution of the blade appeared to be well enough preserved that the induced inflow, and hence the airloads, were computed satisfactorily. But this may turn out to be fortuitous. It is possible that as the grid in the wake is refined and the fidelity of the tip vortex solution improves, the computed blade airloads will become more sensitive to the details of the wake trajectory and structure. This aspect of the hover wake problem clearly warrants further investigation.

Improved Vortex Wake Calculations

The issue of the fidelity of the wake solutions indicates the need for significant improvements in grid resolution and higher-order accuracy in the flow solver. As mentioned above, Dr. Roger Strawn and coworkers are developing solution-adaptive, unstructured-grid subdivision techniques to add grid points selectively in the wake [17,19]. Again, the current model problem is a hovering rotor blade. Initial calculations on a coarse, structured grid are used to determine where to subdivide the computational elements near the edges of the blade and in the wake. Preliminary results for an initial coarse grid are shown in Fig. 10 for the same rotor shown earlier in Figs. 8 and 9. Results with adaptive-grid refinement in the wake will be presented in Ref. 19.

As the wake structure is essentially inviscid, Strawn and Barth [19] have only solved the Euler equations for this problem up to now. The computational cost per time step per grid point is greater with this approach than with the structured-grid TURNS code. However, the efficiency gained by adding and deleting grid points only where they are needed, based on the errors in the local solution, promises to provide an improved resolution of the wake structure at a net savings in computer costs.

An alternative solution-adaptive scheme using structured grids is being developed and applied to the rotor wake problem by Earl P.N. Duque [30]. He is using the Chimera overlapped multiple-grid method [16] at the interface between various structured-grid blocks, each of which is designed to capture a particular region or feature of the flow. Figure 11 shows preliminary results for the same two-bladed rotor in hover, using three coarse-grid blocks. One grid block is fitted to each blade, to capture the flow features near the blades, and these rotate with a third global block, which has grid clustering designed to convect the wake with minimum dissipation. Essentially, the embedded rotor grids act like internal boundary conditions to the cylindrical wake grid, and the wake grid acts like a far-field boundary condition to the blade-fixed grids. Additional calculations will be presented in Ref. 30.

Blade-Vortex Interaction (BVI)

The interaction of a rotor blade with the trailing tip vortex of another is a common event for helicopters, and this interaction is an important source of noise and vibrations. The contributions of two-dimensional Navier-Stokes computations to this problem were reviewed in Refs. 5 and 31. At that time, the near-field properties of airfoil-vortex interaction appeared to be well understood and properly accounted for in numerical simulations. Since then, Baeder [32] has completed a detailed study of the acoustic field generated by 2-D interactions of a prescribed vortex with an airfoil, concluding that the Mach number, vortex strength, and miss distance are the

most important parameters affecting the radiated noise. His results indicate that the noise is relatively independent of the airfoil geometry, thus contrasting with the hopes of many in the helicopter community, who continue to search for a low-BVI-noise blade section. Definitive experiments to settle this issue are planned for the near future at the Ames Research Center.

Three-dimensional interactions of a prescribed vortex with a rotor blade were computed by Srinivasan and McCroskey [33] using an early version of the TURNS code. Representative results are shown in Fig. 12. The test case here is a two-bladed rotor downstream of the tip of a wing in a wind tunnel [34]. The rotor is nominally nonlifting, except for the interaction with the concentrated vortex generated by the wing tip upstream. In this configuration, the approaching vortex is well defined experimentally, and this structure is prescribed in the computations; thus the modeling or computing of the conventional helicopter rotor wake is not an issue here.

For the conditions of Fig. 12, the flow field near the blade tip develops a shock wave on the advancing blade before the blade-vortex encounter in the second quadrant of the rotor, and the decay of this shock is intertwined with the interaction shown in the figure. The calculations agree fairly well with the measurements. This oblique BVI is qualitatively similar to 2-D or "parallel" interactions in many ways, but important quantitative differences exist. Namely, the interaction is spread out over a larger azimuthal travel of the blade, and the fluctuating loads at a given radial station appear to be weaker.

Although further refinements in these Navier-Stokes computations are desirable, the main unresolved issue in computing 3-D BVI is now the accurate simulation of the vortical structures approaching the blade. That is, improvements in the vortex wake calculations, as discussed in the previous section, have become the pacing item in this important aspect of rotor aerodynamics.

IV. ROTOR ACOUSTICS USING CFD

Impulsive-like pressure fluctuations that radiate from rotor blades represent an annoying source of noise that is difficult to calculate. One major source of impulsive noise is the blade-vortex interaction (BVI) phenomena described above; its accurate prediction depends on both the correct description of the vortical wake approaching a blade element and on the local details of the interaction itself. Another source is called High-Speed Impulsive (HSI) noise, which is caused primarily by compressibility effects. It can be accentuated by the phenomenon on transonic rotor tips known as delocalization, wherein the supersonic pocket on the rotor blade extends to the far field beyond the blade tip.

The influence of rotor lift and wakes on HSI noise is considered secondary [35], and Srinivasan and Baeder [36] have indicated that viscous effects are also secondary. Therefore, this source of noise can be investigated for nonlifting transonic configurations using an Euler formulation. On the other hand, the level of the radiated pressure fluctuations drops off inversely with the distance from the effective source, so that the real noise gets quickly lost in the "computational noise" away from the body unless special precautions are taken in the numerics.

Baeder [36-38] has combined high-order-accurate versions of the Euler TURNS code with the special grid-cluster techniques illustrated in Fig. 2 to produce new, high-precision, unified aerodynamic and acoustic results for HSI cases, out to several rotor radii. Some of his hover results are shown in Figs. 13 and 14. These results are the most successful to date for both waveform and peak pressure levels over a range of tip Mach numbers. They are now available as computational data bases, with greater detail and precision than available experimental results, for use by acousticians developing simpler, more approximate theories and models.

Forward flight is more challenging, as the solutions must be time accurate, and the characteristics along which the outgoing waves propagate are no longer fixed with respect to the blade. Nevertheless, Baeder [37] has used the TURNS code and grid clustering along selected linear characteristics to begin to investigate rotors in forward flight at tip-Mach-number conditions below and above that required for delocalization. The overall picture of the wave propagation for a nonlifting, untwisted rotor blade agrees well with what can be qualitatively inferred from wind tunnel measurements. Detailed comparisons have been made with experiments at specific microphone locations away from the rotor, as shown in Fig. 15, with good results for the case without delocalization.

The quantitative agreement is less satisfactory at advancing-tip Mach numbers above delocalization, as shown in Fig. 16, where the acoustic waves seem to be more sensitive to the basic parameters of the rotor. It should be noted that the measurements shown in the figure were obtained for lifting rotors with twisted blades. Also, there is some disagreement between measurements in a wind tunnel and those obtained in flight tests; these differences are discussed in Ref. 39. In any case, Baeder's calculations represent a significant advance, and they demonstrate the feasibility of using a unified CFD approach to examine nonlinear acoustics of rotors. However, they also suggest that further validation should be done for additional cases, that the actual blade conditions should be modeled more exactly, and that improvements in time-varying grids, including solution-adaptive techniques, will probably be required to obtain the quality of the hover results in Figs. 13-14.

V. TOWARD ROTOR-BODY INTERACTIONS

The aerodynamic interaction between rotating and nonrotating components of rotary-wing aircraft is widely recognized as an important feature that produces considerable additional complications for CFD analyses. Unfortunately, measurable progress on this important topic has been slow, consisting mostly of conceptualizing and developing viable grid-interface strategies.

However, as an intermediate step, Dr. Sharon Stanaway has developed an efficient method for embedding an actuator-disk representation of a rotor in a computational domain surrounding an arbitrary body. The method uses the Fortified Navier Stokes technique of Van Dalsem and Steger [40] to introduce a prescribed pressure jump, which may vary with time and space, across an internal boundary (the actuator disk). This is similar to the work of Rajagopalan [10], in which a momentum source term is added to the governing equations, causing a pressure jump at internal boundary points. The technique is intended to allow simplified

studies of the effect of the wake of a rotor on a nearby fuselage or wing, for example. The actuator disk will eventually be replaced by a finite-difference simulation of the rotor, as indicated in Fig. 17. A number of fuselage calculations have been performed in support of the rotor-body experiment of Norman and Yamauchi [41], but these have not been completed.

Another unpublished early application of this technology by Dr. Stanaway is illustrated in Fig. 18. This ducted-rotor model problem is an approximation of the novel Sikorsky Cypher unmanned aerial vehicle [42], which resembles a flying doughnut with two counterrotating rotors. The figure shows Mach contours on planes taken through the center of a toroidal body of circular cross section, with and without a thrusting rotor system spanning the inside of the toroid. The direction of the oncoming flow is indicated in the figure; the flow fields are axisymmetric in this example of vertical climb. The solution without the actuator disk, in the left half of the figure, exhibits the expected behavior of a pair of circular cylinders in a two-dimensional crossflow. The effect of the thrusting rotor is to accelerate the flow through the middle of the toroid, to move the stagnation point inward, and to alter the pressure distribution and separation point location significantly.

In a third preliminary and unpublished study, Dr. Venkat Raghavan is adapting the OVERFLOW code to the V-22 Osprey tiltrotor aircraft, with initial emphasis on the high-speed cruise configuration, or turboprop mode, of this vehicle. Figure 19 illustrates the surface and volume grids being developed for this problem, using OVERFLOW with Chimera. Progress to date includes full-potential and Navier-Stokes solutions for the wing-fuselage combination. The viscous results (not shown) demonstrate separated flow on the rear portion of the lower fuselage, whereas the inviscid results do not, of course. The addition of the aforementioned actuator-disk representation of the rotor is the next logical step in this progression toward a simulation of the complete aircraft.

VI. CONCLUDING REMARKS

This paper has attempted to describe the progress made in the last four years by the author and his coworkers, and some of the current limitations and problems. As one of several teams actively working in the field of rotorcraft CFD, we are pursuing the Euler/Reynolds-Averaged Navier-Stokes approach, with growing emphasis on rotor wakes and rotor-body interactions. The examples shown are mostly for the aerodynamics and acoustics of rotors in hover, but the primary long-term goal is to develop improved predictive capability for forward flight. Solution-adaptive structured- and unstructured-grid methods are under development for improved wake capturing and acoustics, and variations on the Chimera overset grid scheme appear to be the most promising ways of treating rotor-body interactions.

In concluding his 1988 review [5], the author wrote, "The rotorcraft industry appears to be entering a new era in which computational fluid dynamics will play an increasingly important role in the design and analysis of advanced aircraft." Although the extent of CFD contributions to the new rotary-wing aircraft that have appeared since then may not have been overwhelming, the number of rotorcraft CFD papers in the technical literature by industry authors has risen dramatically. Since 1988, airfoil codes have improved significantly and are being used more. Also, the transonic aerodynamics of advancing-blade tips is being computed by a variety of methods with adequate precision for engineering applications, and these capabilities are beginning to be used in industry. Furthermore, accurate simulation of high-speed impulsive noise within a few radii from the tip of the blade now appears to be possible in those cases where wake effects are negligible. A logical next step is to try to extend this capability to the more difficult problem of blade-vortex interaction noise.

There has also been significant progress in CFD algorithms, grid techniques, and supercomputer technology during the past four years. However, much remains to be done in each of these areas to bring CFD to the state where it can be used as successfully for rotorcraft as for fixed wing aircraft. An accurate finite-difference simulation of the complete flow field about a helicopter is still not feasible. Wakes and blade-vortex interactions are not well predicted, and retreating-blade stall remains virtually untouched by the CFD community. The principal limitations remain the computer hardware costs, speeds, and memory capacities; algorithms and solution methods; grid generation; turbulence models; and accurate vortex-wake simulations. In general, today's rotorcraft CFD codes are not robust, they have not been exercised enough nor validated adequately, and they remain awkward to use. All of these factors undoubtedly discourage the user community from working with what is available. Nevertheless, the technical challenges are exciting and the potential payoff of future CFD developments remains well worth pursuing.

VII. ACKNOWLEDGEMENTS

This paper draws heavily from the research activities of my coworkers, J.D. Baeder, E.P.N. Duque, V. Raghavan, G.R. Srinivasan., S. Stanaway, and R.C. Strawn. Their ideas and contributions are gratefully acknowledged. Also, hover-wake information provided by Dr. Chee Tung was instrumental in developing the new outer boundary conditions described in Section III, and his cooperation is deeply appreciated.

VIII. REFERENCES

1. Caradonna, F.X. "The Application of CFD to Rotary Wing Flow Problems," Paper No. 5, AGARD Report 781, Nov. 1990.
2. Caradonna, F.X., and Tung, C. "A Review of Current Finite-Difference Rotor Flow Methods," American Helicopter Society 42nd Annual Forum, June 1986.
3. Strawn, R.C., Desopper, A., Miller, J., and Jones, A. "Correlation of Puma Airloads - Evaluations of CFD Prediction Methods," 15th European Rotorcraft Forum, Amsterdam, Sept. 1989.
4. Polz, G. "Current European Rotorcraft Research Activities on Development of Advanced CFD Methods for the Design of Rotor Blades," 17th European Rotorcraft Forum, Berlin, Sept. 1991.
5. McCroskey, W.J. "Some Rotorcraft Applications of Computational Fluid Dynamics," Second International Conference on Basic Rotorcraft Research, Univ. Maryland, Feb. 1988; also NASA TM 100067, 1988.

6. Wake, B.E., and Egolf, T.A. "Application of a Rotary-Wing Viscous Flow Solver on a Massively-Parallel Computer," AIAA Paper 90-0334, Reno, Jan. 1990.

7. Agarwal, R.K., and Deese, J.E., "Euler/Navier-Stokes Calculations for the Flowfield of a Helicopter Rotor in Hover and Forward Flight," Proc. Second International Conference on Rotorcraft Basic Research, Univ. Maryland, Feb. 1988.

8. Scott, M.T., and Narramore, J.C. "Navier-Stokes Correlation of a Swept Helicopter Rotor Tip at High Alpha," AIAA Paper 91-1752, Honolulu, June 1991.

9. Aoyama, T., Saito, S. and Kawachi, K. "Navier-Stokes Analysis of Blade Tip Shape in Hover," 16th European Rotorcraft Forum, Glasgow, Sept. 1990.

10. Rajagopalan, R.G., and Mathur, S.R. "Three-Dimensional Analysis of a Rotor in Forward Flight," American Helicopter Society 47th Annual Forum, Phoenix, May 1991.

11. Anderson, D.A., Tannehill, J.C., and Pletcher, R.H. Computational Fluid Mechanics and Heat Transfer, McGraw-Hill, 1984, pp. 421-424.

12. Srinivasan, G.R., Baeder, J.D., Obayashi, S., and McCroskey, W.J. "Flowfield of a Lifting Hovering Rotor - A Navier-Stokes Simulation," 16th European Rotorcraft Forum, Glasgow, Sept. 1990.

13. Obayashi, S. "Numerical Simulation of Underexpanded Plumes Using Upwind Methods," AIAA Paper 88-4360-CP, Minneapolis, Aug. 1988.

14. Ying, S.X., Steger, J.L., Schiff, L.B., and Baganoff, D. "Numerical Simulation of Unsteady, Viscous, High Angle of Attack Flows Using a Partially Flux-Split Algorithm," AIAA Paper 86-2179, Williamsburg, Aug. 1986.

15. Pulliam, T.H., and Chaussee, D.S. "A Diagonal Form of a Implicit Approximate-Factorization Algorithm," J. Computational Physics, Vol. 39, No. 2, Feb. 1981, pp. 347-363.

16. Steger, J.L., Dougherty, F.C., and Benek, J.A. "A Chimera Grid Scheme," Advances in Grid Generation, K.N. Ghia and U. Ghia, eds., ASME FED Vol. 5, 1983, pp. 59-69.

17. Strawn, R.C. "Wing-Tip Vortex Calculations with an Unstructured Adaptive-Grid Euler Solver," American Helicopter Society 47th Annual Forum, Phoenix, May 1991.

18. Barth, T.J. "A 3-D Upwind Euler Solver for Unstructured Meshes," AIAA Paper 91-1548, Honolulu, June 1991.

19. Strawn, R.C., and Barth, T.J. "A Finite-Volume Euler Solver for Computing Rotary-Wing Aerodynamics on Unstructured Meshes," American Helicopter Society 48th Annual Forum, Washington, June 1992.

20. G.R. Srinivasan, W.J. McCroskey, J.D. Baeder, and T.A. Edwards, "Numerical Simulation of Tip Vortices of Wings in Subsonic and Transonic Flow," AIAA Journal, Vol. 26, No. 10, Oct. 1988, pp 1153-1162.

21. McAlister, K.W., and Takahashi, R.K. "NACA 0015 Wing Pressure and Trailing Vortex Measurements," NASA TP 3151, Aug. 1991.

22. Chow, J.S., Zilliac, G.G., and Bradshaw, P. "Initial Roll-Up of a Wingtip Vortex," FAA International Wake-Vortex Symposium, Washington, Oct. 1991.

23. E.P.N. Duque, "A Numerical Analysis of the BERP Blade," American Helicopter Society 45th Annual Forum, May 1989; also NASA TM 102247, 1989.

24. Brocklehurst, A., and Duque, E.P.N., "Experimental and Numerical Study of the British Experimental Rotor Program Blade," AIAA Paper 90-3008, Portland, Aug. 1990.

25. G.R. Srinivasan and W.J. McCroskey, "Navier-Stokes Calculations of Hovering Rotor Flowfields," Journal of Aircraft, Vol. 25, No. 10, Oct. 1988, pp. 865-875.

26. C.L. Chen and W.J. McCroskey, "Euler Solution of Multiblade Rotor Flow," Vertica, Vol. 12, No. 3, Mar. 1988, pp. 303-313.

27. C.L. Chen and W. J. McCroskey, "Numerical Simulation of Helicopter Multi-Bladed Rotor Flow," AIAA Paper 88-0046, Reno, Jan. 1988.

28. Srinivasan, G.R., Raghavan, V., and Duque, E.P.N., "Flowfield Analysis of Modern Helicopter Rotors in Hover by Navier-Stokes Method," American Helicopter Society International Technical Specialists' Meeting, Philadelphia, Oct. 1991.

29. Hertel, J., Kramer, E., and Wagner, S. "Complete Euler Solution for a Rotor in Hover and a Propeller in Forward Flight," 16th European Rotorcraft Forum, Glasgow, Sept. 1990.

30. Duque, E.P.N. "Numerical Simulation of a Hovering Rotor Blade using Embedded Grids," American Helicopter Society 48th Annual Forum, Washington, June 1992.

31. Srinivasan, G.R., and McCroskey, W.J. "Numerical Simulations of Unsteady Airfoil-Vortex Interactions," Vertica, Vol. 11, No. 1/2, Jan. 1987, pp. 3-28.

32. Baeder, J.D. "The Computation and Analysis of Acoustic Waves in Transonic Airfoil-Vortex Interactions," PhD Thesis, Stanford University, Sept. 1989.

33. G.R. Srinivasan and W.J. McCroskey, "Viscous, Unsteady Interaction of a Rotor with a Vortex," AIAA Paper 89-1848, Buffalo, N.Y., June 1989.

34. Caradonna, F.X., Lautenschlager, J., and Silva, M. "An Experimental Study of Rotor Blade-Vortex Interactions," AIAA Paper 88-045, Reno, Jan. 1988.

35. Schmitz, F.H., and Yu, Y.H. "Helicopter Impulsive Noise: Theoretical and Experimental Status," Recent Advances in Aeroacoustics, ed. A. Krothapalli and C.A. Smith, Springer-Verlag, 1986, pp. 149-243; also NASA TM 84390, Nov. 1983.

36. Srinivasan, G.R., and Baeder, J.D. "Recent Advances in Euler and Navier-Stokes Methods for Calculating Helicopter Rotor Aerodynamics and Acoustics," 4th

International Symposium on Computational Fluid Dynamics, Davis, Sept. 1991.

37. Baeder, J.D. "Euler Solutions to Nonlinear Acoustics of Non-Lifting Hovering Rotor Blades," 16th European Rotorcraft Forum, Glasgow, Sept. 1990.

38. J.D. Baeder, "Euler Solutions to Nonlinear Acoustics of Non-Lifting Rotor Blades in Forward Flight," American Helicopter Society International Technical Specialists' Meeting, Philadelphia, Oct. 1991.

39. Splettstoesser, W.R., Schultz, K.J., Schmitz, F.H., and Boxwell, D.A. "Model Rotor High-Speed Impulsive Noise - Parametric Variations and Full-Scale Comparisons," American Helicopter Society 39th Annual Forum, St. Louis, May 1983.

40. Van Dalsem, W. R., "Study of Jet in Ground Effect with a Crossflow Using the Fortified Navier-Stokes Scheme," AIAA Paper 87-2279-CP, Monterey, Aug. 1987.

41. Norman, T.R., and Yamauchi, G.K. "Full-Scale Investigation of Aerodynamic Interactions between a Rotor and a Fuselage," American Helicopter Society 47th Annual Forum, Phoenix, May 1991.

42. DeMeis, R. "A Cypher That Adds Up," Aerospace America, Vol. 29, No. 1, Jan. 1991, p. 39.

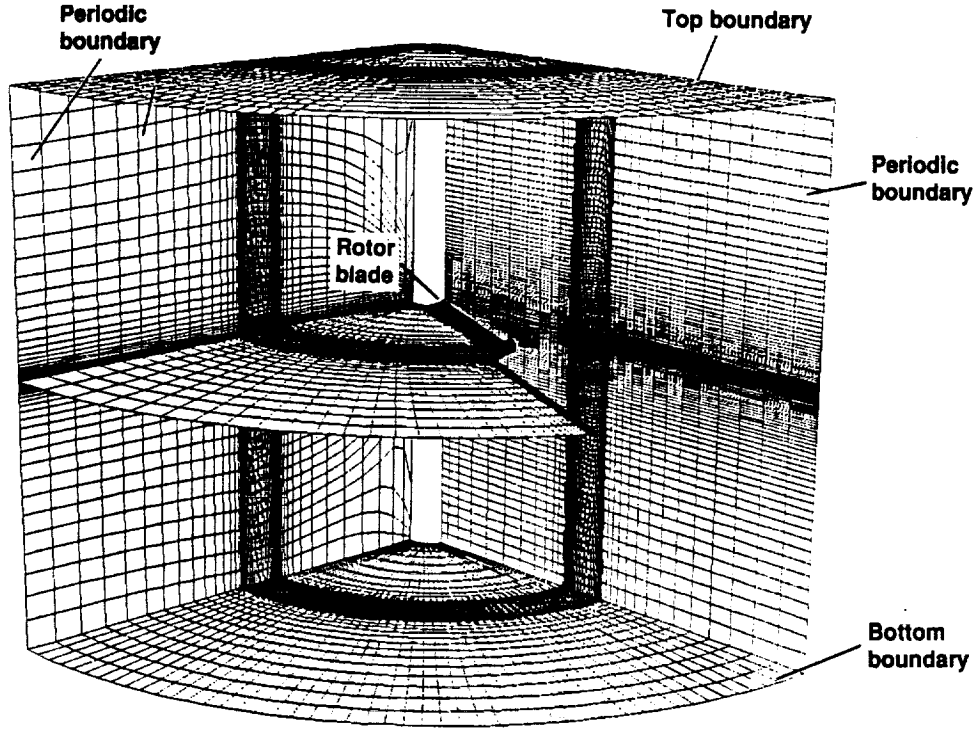

Fig. 1 Representative C-H grid topology for a rotor blade, showing the grid in the plane of the blade.

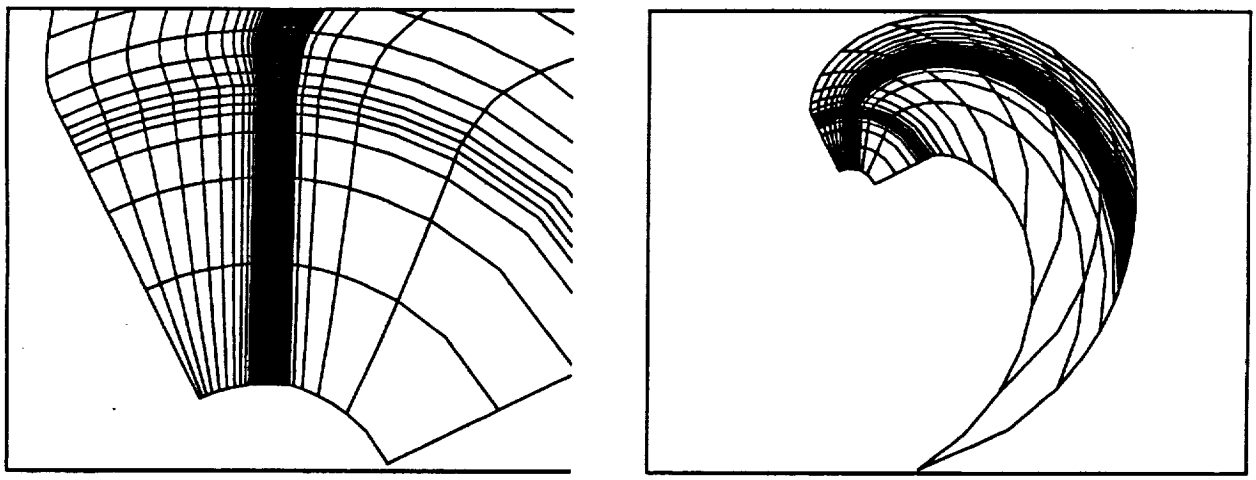

Fig. 2 Representative grid in the plane of the rotor blade for computing acoustic waves.

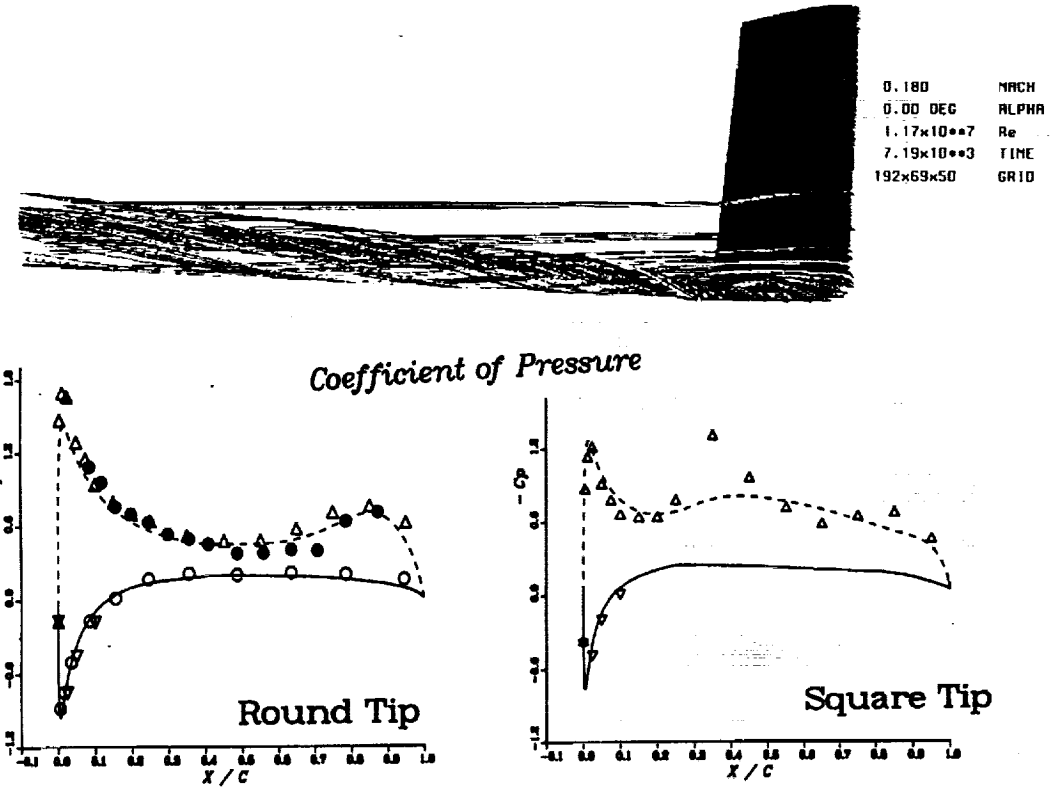

Fig. 3 Pressure distributions and streamlines near the tip of a rectangular wing in subsonic flow

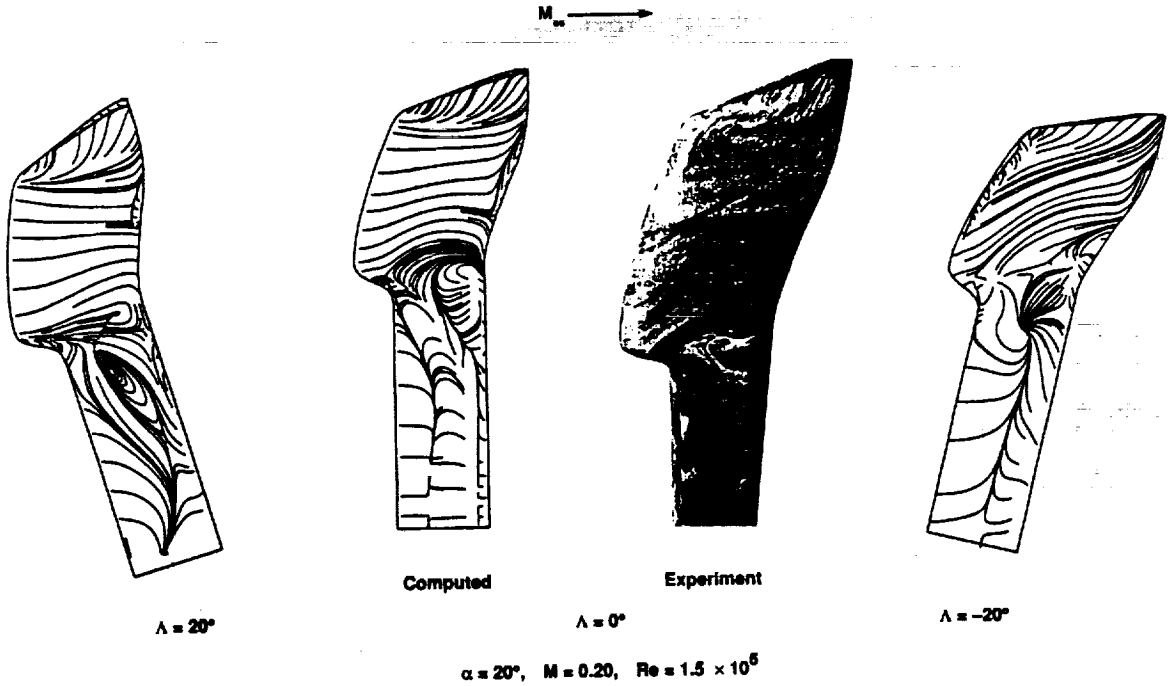

Fig. 4 Surface streamline patterns for a British Experimental Rotor Program blade tip, nonrotating at high incidence and sweep in subsonic flow

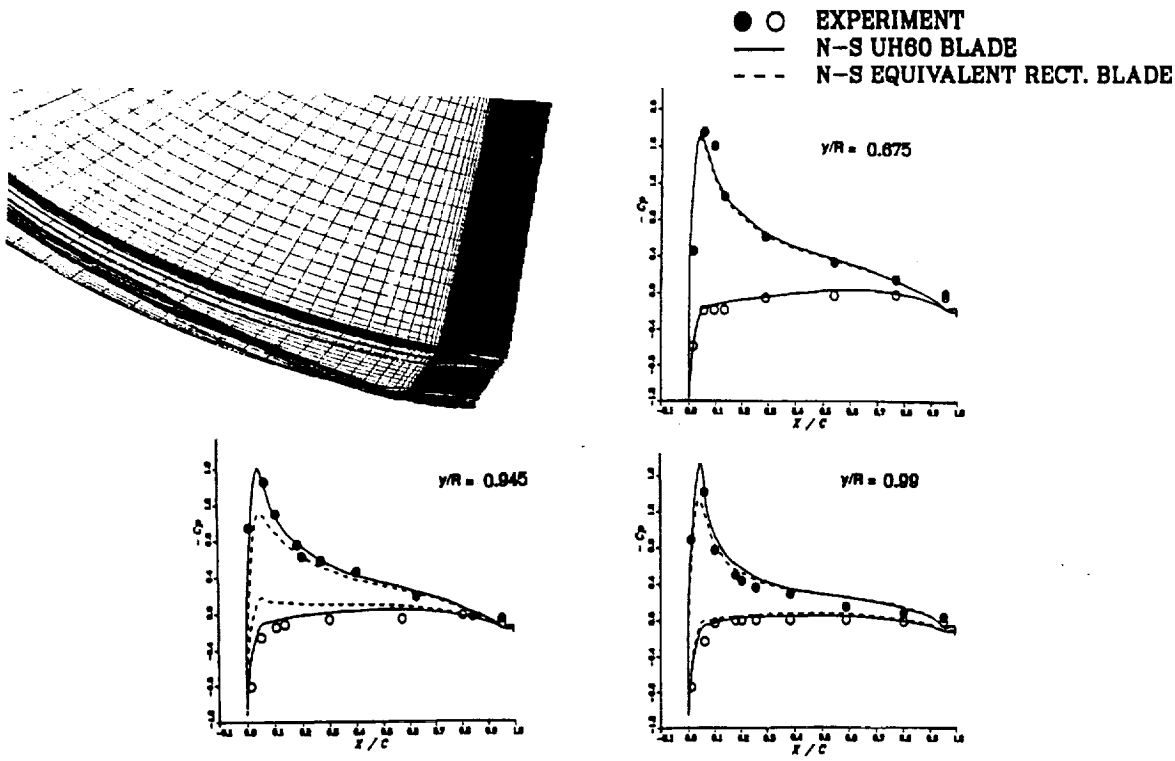

Fig. 5 Pressure distributions and streamlines on a model UH-60A rotor blade in hover

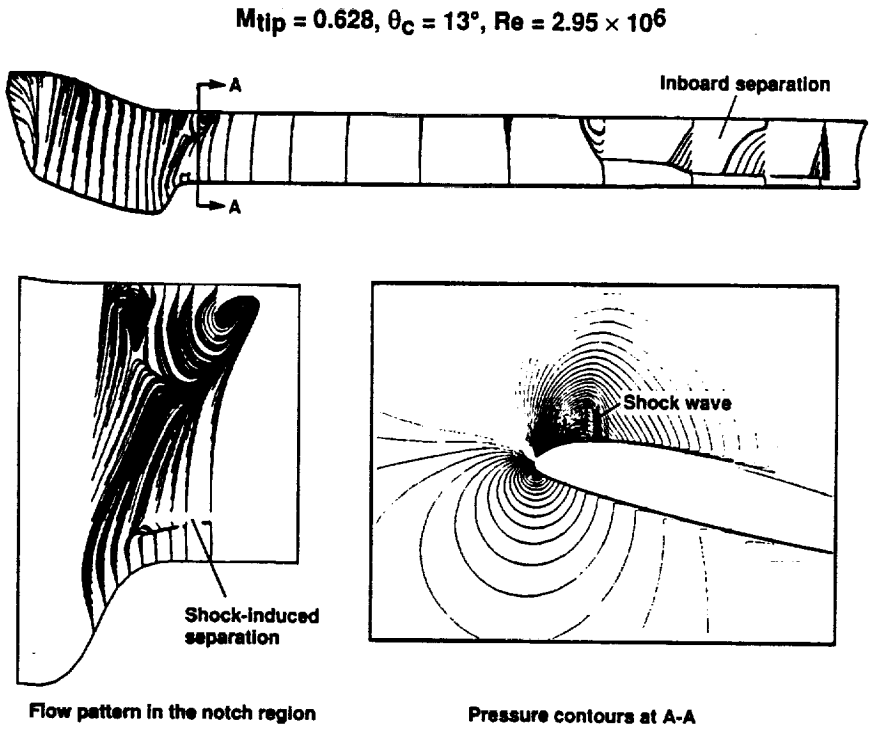

Fig. 6 Surface pressure contours and streamline patterns for a BERP blade in hover

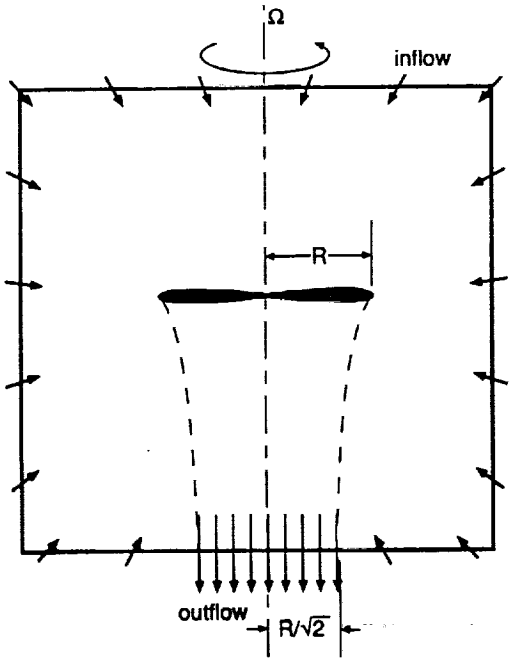

Fig. 7 Sketch of outer boundary conditions used in hover calculations

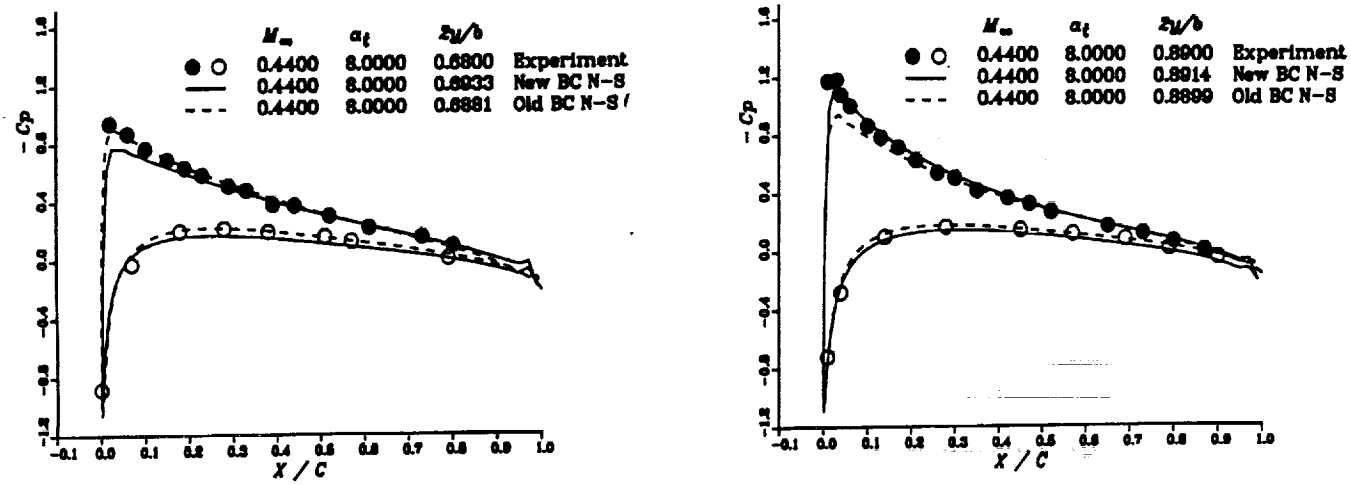

Fig. 8 Pressure distributions on a hovering rotor with original and modified outer boundary conditions.

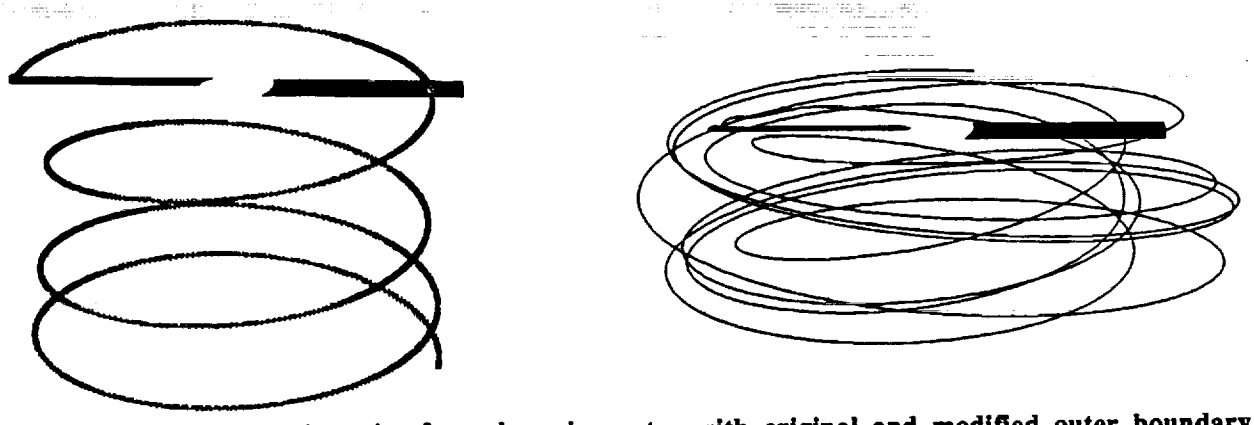

Fig. 9 Tip-vortex particle trajectories for a hovering rotor with original and modified outer boundary conditions.

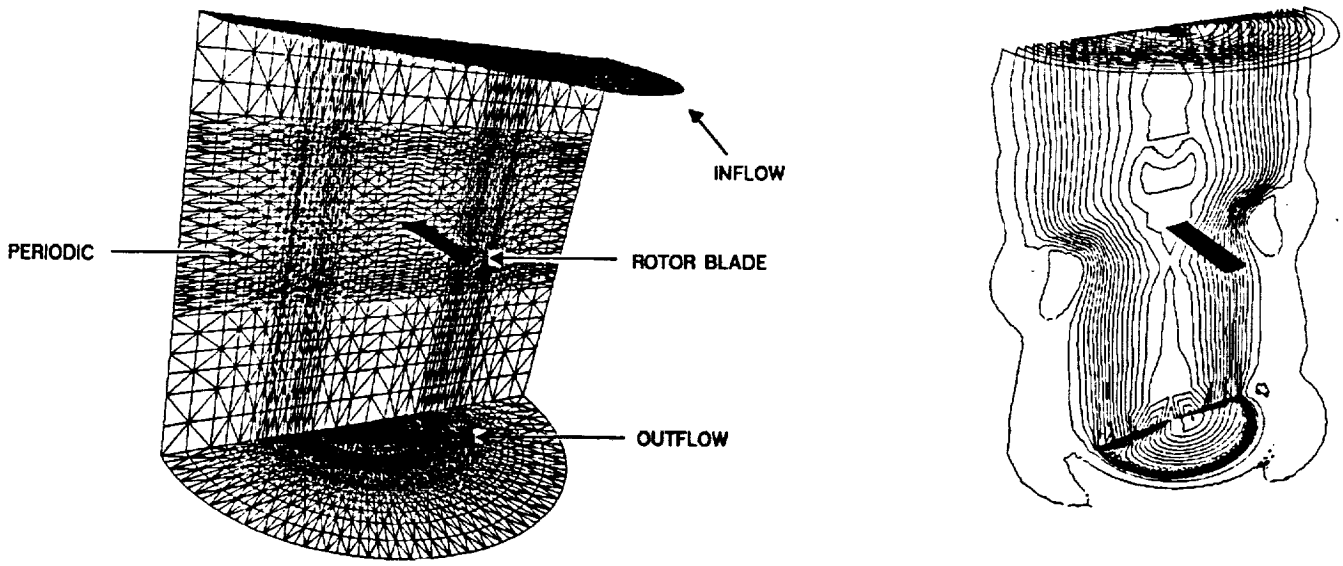

Fig. 10 Initial grid and density contours for an unstructured-grid calculation of a hovering rotor

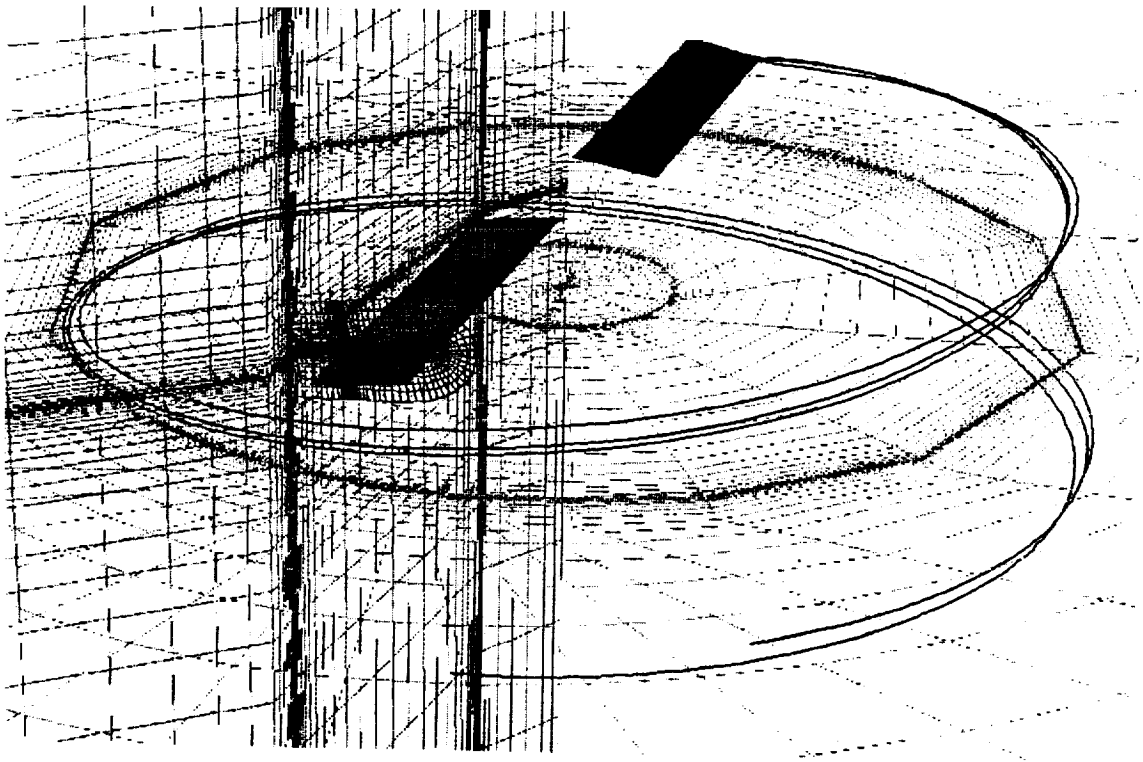

Fig. 11 Grid and vortex trajectory for a three-zone calculation of a rotor in hover

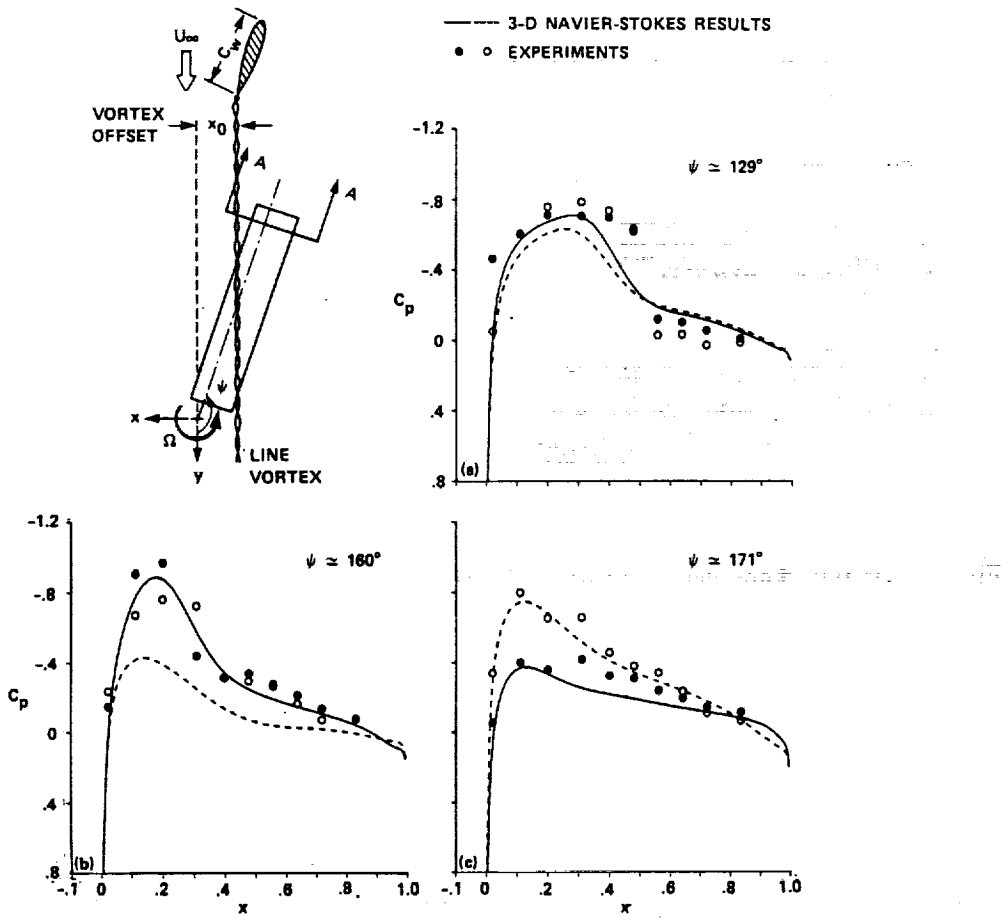

Fig. 12 Unsteady pressure distributions near the tip during an oblique blade-vortex interaction

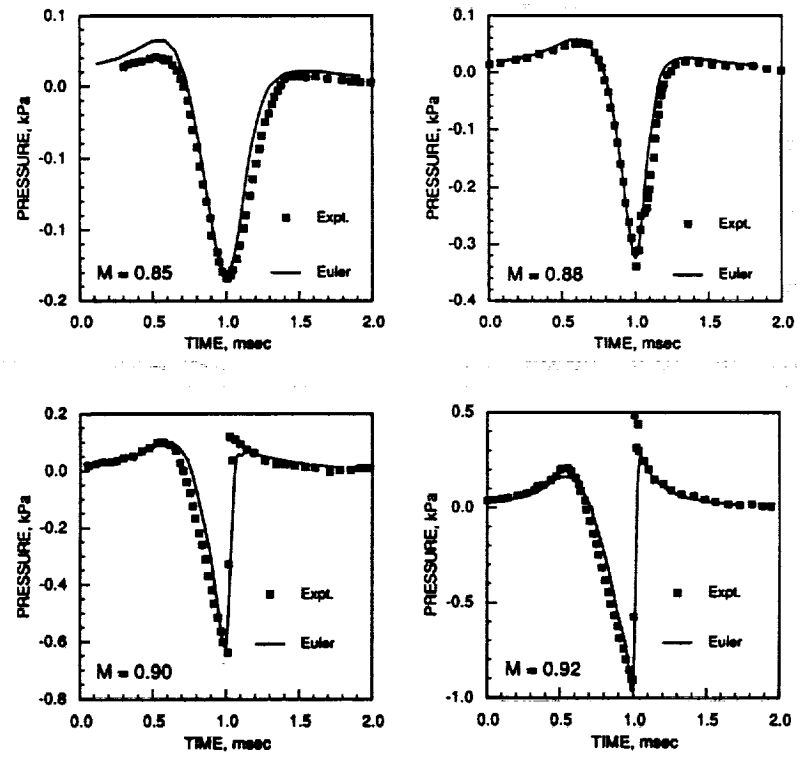

Fig. 13 Pressure time histories in the plane of a hovering rotor at r/R = 3.09 for various tip Mach Numbers

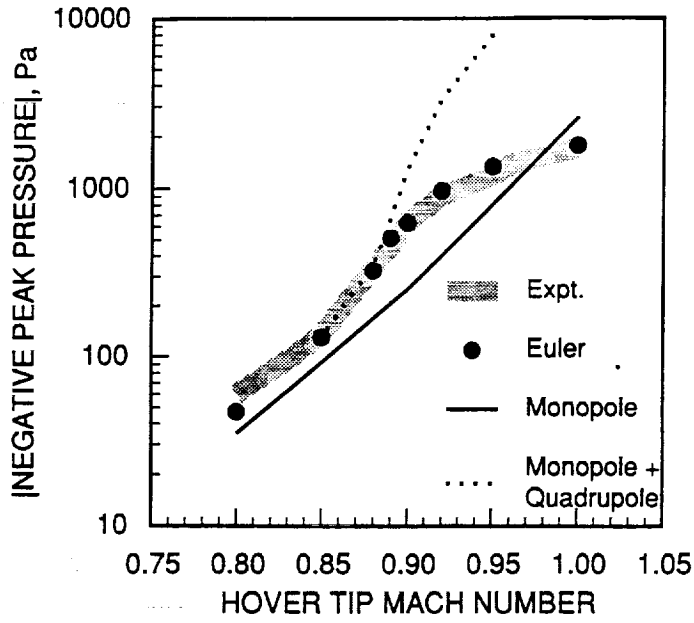

Fig. 14 Magnitude of the acoustic wave of a hovering rotor at r/R = 3.09 for various tip Mach Numbers

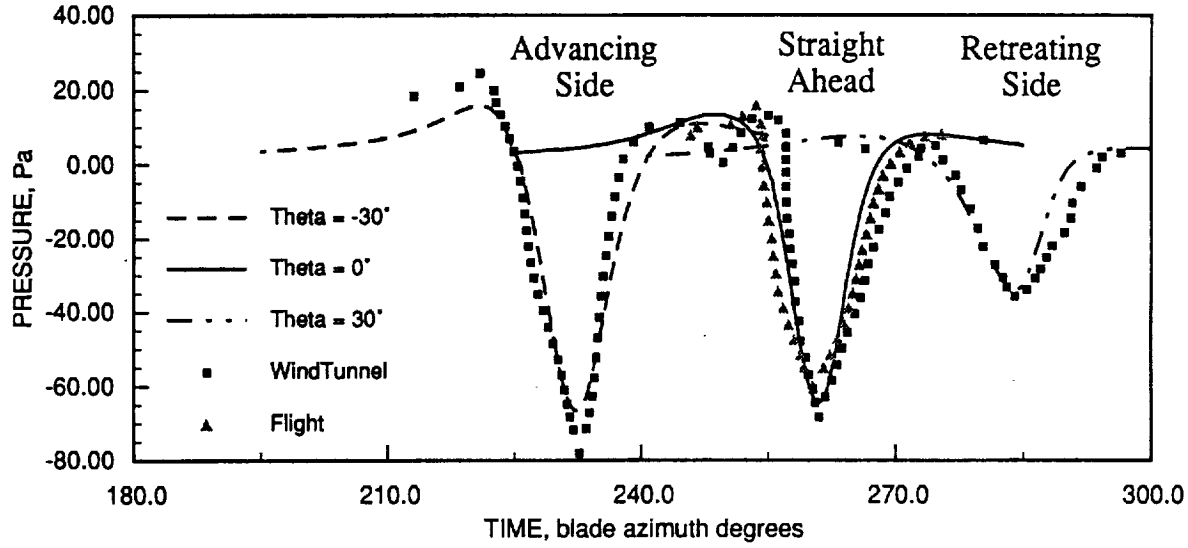

Fig. 15 Pressure time histories in the plane of a rotor in forward flight for maximum tip Mach number = 0.837

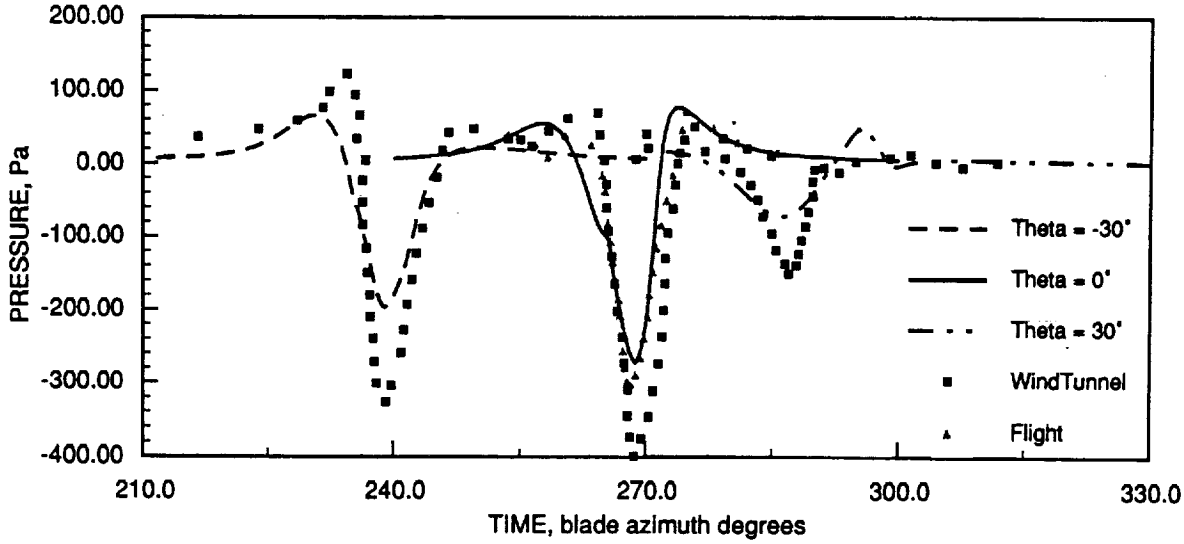

Fig. 16 Pressure time histories in the plane of a rotor in forward flight for maximum tip Mach number = 0.896

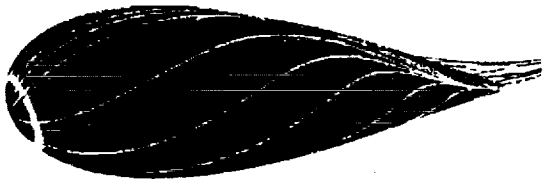

(a) Navier Stokes calculation on an isolated body (turbulent flow, Re=27,000,000, alpha=17 deg., M=0.18)

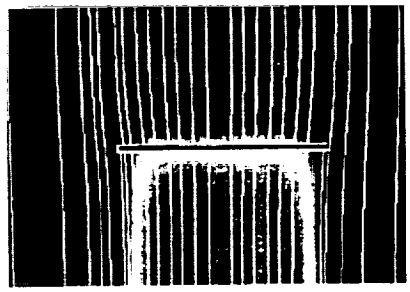

(b) Horizontal slice through an actuator disk rotor simulation of the Navier Stokes equations

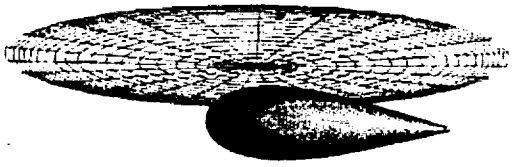

(c) Body and rotor are combined using overset grids (Chimera/ F3D).

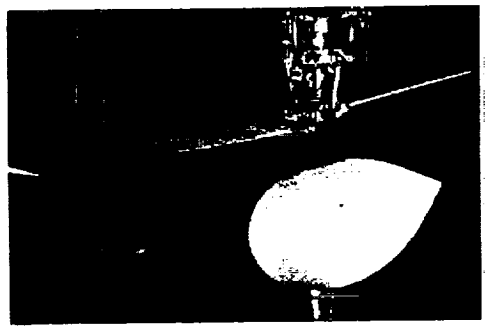

(d) 7 by 10 foot rotor-body interference wind tunnel test.

Fig. 17 Combination of components for studying rotor-body interactions

Fig. 18 Actuator-disk model of a toroidal ducted rotor.

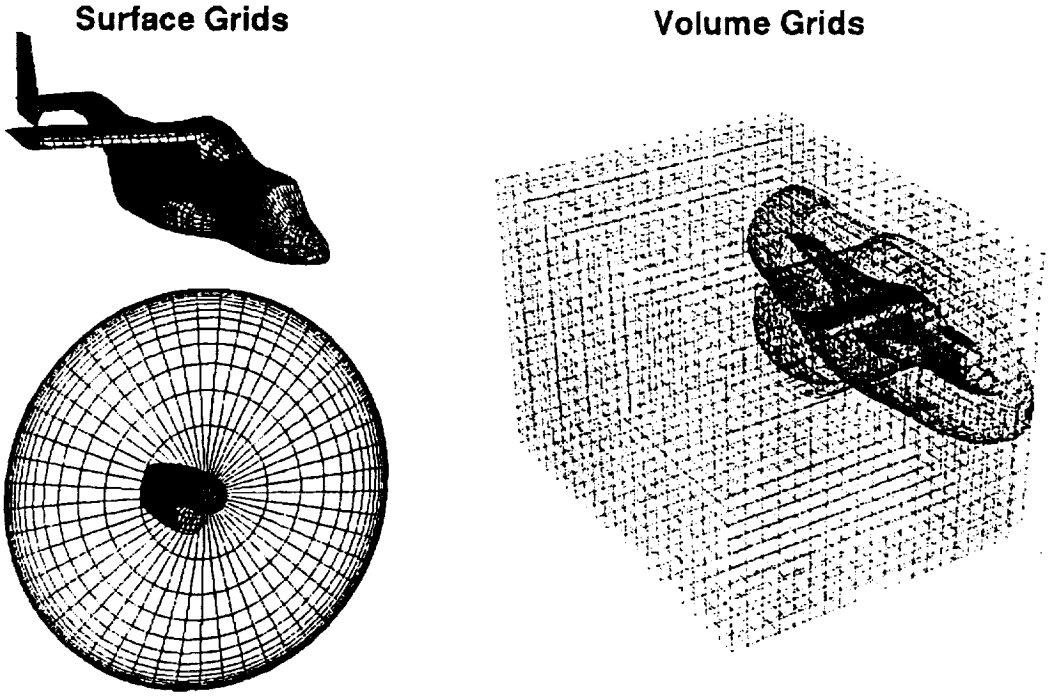

Fig. 19 Chimera multi-block grid topology for tiltrotor aircraft.